

Transport and magnetic properties of $\text{Ru}(\text{Sr}_{1-x}\text{La}_x)_2\text{RCu}_2\text{O}_8$ (R = Gd, Eu) superconductor

A. Hassen, Prabhat Mandal, Joachim Hemberger, Alexander Krimmel, P. Choudhury, B. Ghosh, Alois Loidl

Angaben zur Veröffentlichung / Publication details:

Hassen, A., Prabhat Mandal, Joachim Hemberger, Alexander Krimmel, P. Choudhury, B. Ghosh, and Alois Loidl. 2003. "Transport and magnetic properties of $\text{Ru}(\text{Sr}_{1-x}\text{La}_x)_2\text{RCu}_2\text{O}_8$ (R = Gd, Eu) superconductor." *Physica. C* 398 (3-4): 123–30.
[https://doi.org/10.1016/S0921-4534\(03\)01273-5](https://doi.org/10.1016/S0921-4534(03)01273-5).

Transport and magnetic properties of $\text{Ru}(\text{Sr}_{1-x}\text{La}_x)_2\text{RCu}_2\text{O}_8$ ($\text{R} = \text{Gd}, \text{Eu}$) superconductor

A. Hassen ^a, P. Mandal ^{b,*}, J. Hemberger ^a, A. Krimmel ^a, P. Choudhury ^c,
B. Ghosh ^b, A. Loidl ^a

^a *Experimentalphysik V, EKM, Universität Augsburg, D-86135 Augsburg, Germany*

^b *Saha Institute of Nuclear Physics, ECMP Division, 1/AF Bidhanagar, Calcutta 700 064, India*

^c *Central Glass and Ceramic Research Institute, 196 Raja S. C. Mullick Road, Calcutta 700 032, India*

Received 24 April 2003; accepted 6 May 2003

The recent discovery [1–4] of superconductivity in layered ruthenate–cuprate compounds $\text{RuSr}_2\text{RCu}_2\text{O}_8$ ($\text{R} = \text{Gd}$ and Eu) is a subject of intense interest as a unique model system for studying the interplay between superconductivity and ferromagnetism. Superconductivity and magnetism are two different ordered states and are inimical to one another. In conventional s-wave superconductor, both the local magnetic moments of the impurity ions and the external magnetic field break up the

spin singlet Cooper pairs and hence suppress superconductivity which is known as pair breaking effect. In $\text{RuSr}_2\text{GdCu}_2\text{O}_8$ (RuGd-1212) compound, a small amount of ferromagnetic (FM) moment in the RuO_2 layers coexists with a bulk superconductivity originated in the CuO_2 bilayers over a wide range of temperature [5,6]. The magnetic transition occurs at $T_M = 132$ K which is considerably higher than the superconducting onset temperature $T_c^{\text{on}} = 46$ K. The neutron diffraction and magnetization measurements [7–9] suggest that the Ru moment orders predominantly antiferromagnetically along the c -axis with spin canting within the ab -plane. At zero field the net in-plane FM moment is about $0.05 \mu_B/\text{Ru}$,

* Corresponding author. Tel.: +91-33-23375345; fax: +91-33-23374637.

E-mail address: mandal@cmp.saha.ernet.in (P. Mandal).

which increases with external magnetic field and the system becomes FM at high fields [10]. Additionally, normal-state transport [5] and thermodynamic properties [5] and infrared (IR) conductivity [11] measurements show that $\text{RuSr}_2\text{RCu}_2\text{O}_8$ behaves as a typical underdoped superconducting cuprate and exhibits a number of features arising due to the presence of a pseudogap in the excitation spectrum of the density of states.

High temperature superconductors (HTSC) are known to undergo insulator-to-superconductor-to-normal metal transition as the hole concentration (p) increases continuously with doping. Superconductivity usually occurs over a narrow range of p and there is an optimum doping level (p_{op}) at which highest T_c (T_c^{max}) is realized. The material is underdoped for $p < p_{\text{op}}$, where T_c increases with doping, and overdoped for $p > p_{\text{op}}$, where it becomes a better metal and behaves like a Fermi liquid as the hole doping progresses but T_c decreases monotonically. The hole doping phenomenon establishes a parabolic relation [12] between T_c and p which is symmetric about p_{op} . To understand the occurrence of superconductivity and the unusual normal-state properties, the systematic trends of evolution of various physical properties with doping have been sought for in these systems.

Usually there are two standard methods to change the carrier density in HTSC, either by tuning the oxygen content through annealing and subsequently quenching from different temperatures or by substituting the divalent ion with the trivalent rare-earth ion and vice versa. The former method was found to be quite suitable for $\text{YBa}_2\text{Cu}_3\text{O}_{7-\delta}$ (Y-123) and other cuprate systems. In RuGd-1212 , the thermopower S which is a measure of carrier density does not change significantly with long time annealing in flowing oxygen but the zero-resistance temperature, T_c ($R = 0$) changes appreciably [5]. It has also been observed that annealing and then quenching from different temperatures do not change the oxygen content and superconducting onset temperature but affects the granularity, and hence the transition width. Thus this method is not suitable to change the carrier density in ruthenate-cuprates.

In this paper we report systematic variation of resistivity, magnetoresistance, magnetization and thermoelectric power in $\text{Ru}(\text{Sr}_{1-x}\text{La}_x)_2\text{RCu}_2\text{O}_8$ for $0 \leq x \leq 0.10$ in which carrier density has been reduced by substituting Sr partially with La ion. We also compare the observed results with other HTSC.

Polycrystalline samples have been synthesized by solid-state reaction method [5] using high purity RuO_2 , SrCO_3 , La_2O_3 , R_2O_3 , CuO and ZnO powders. At the final stage, the samples were annealed for 6 days at 1060°C in flowing oxygen followed by slow cooling to room temperature. X-ray diffraction shows that the Gd-based samples are single phase with tetragonal structure [10]. Samples with $x > 0.10$ show impurity peaks and hence, not included in this study. Eu-based samples show a weak impurity peak at around $2\theta = 31.5^\circ$ similar to that reported by others [13]. Magnetic susceptibility was measured using a SQUID magnetometer (Quantum Designs, MPMS). Resistance and magnetoresistance measurements were performed by conventional four-probe technique under magnetic fields up to 14 T in a superconducting magnet (Oxford Instruments). The thermopower was measured from 325 to 77 K by an automated standard dc method using a differential technique.

Fig. 1 shows the resistivity $\rho(T)$ behavior for the $\text{RuSr}_2\text{RCu}_2\text{O}_8$ samples with different x . The temperature dependence of ρ for RuGd-1212 is similar to that reported by Tallon et al. [5]. ρ decreases slowly with lowering temperature, passes through a shallow minimum at around $T^* = 87$ K and then increases slowly before it drops sharply below 46 K. T_c ($R = 0$) for this sample is 31 K. This kind of minimum in $\rho(T)$ has also been observed in other underdoped HTSC in the vicinity of insulator to metal transition point [14]. With the substitution of La for Sr, normal as well as superconducting state properties change systematically with x . Only 1% La substitution suppresses superconducting transition temperature drastically. For $x = 0.01$ sample, T_c^{on} and T_c ($R = 0$) are 33 and 14 K, respectively. Thus, La doping reduces T_c considerably and broadens the resistive transition, characteristic of underdoped cuprates. However, the evolution of both normal and superconducting state properties in RuGd-1212 with La doping are

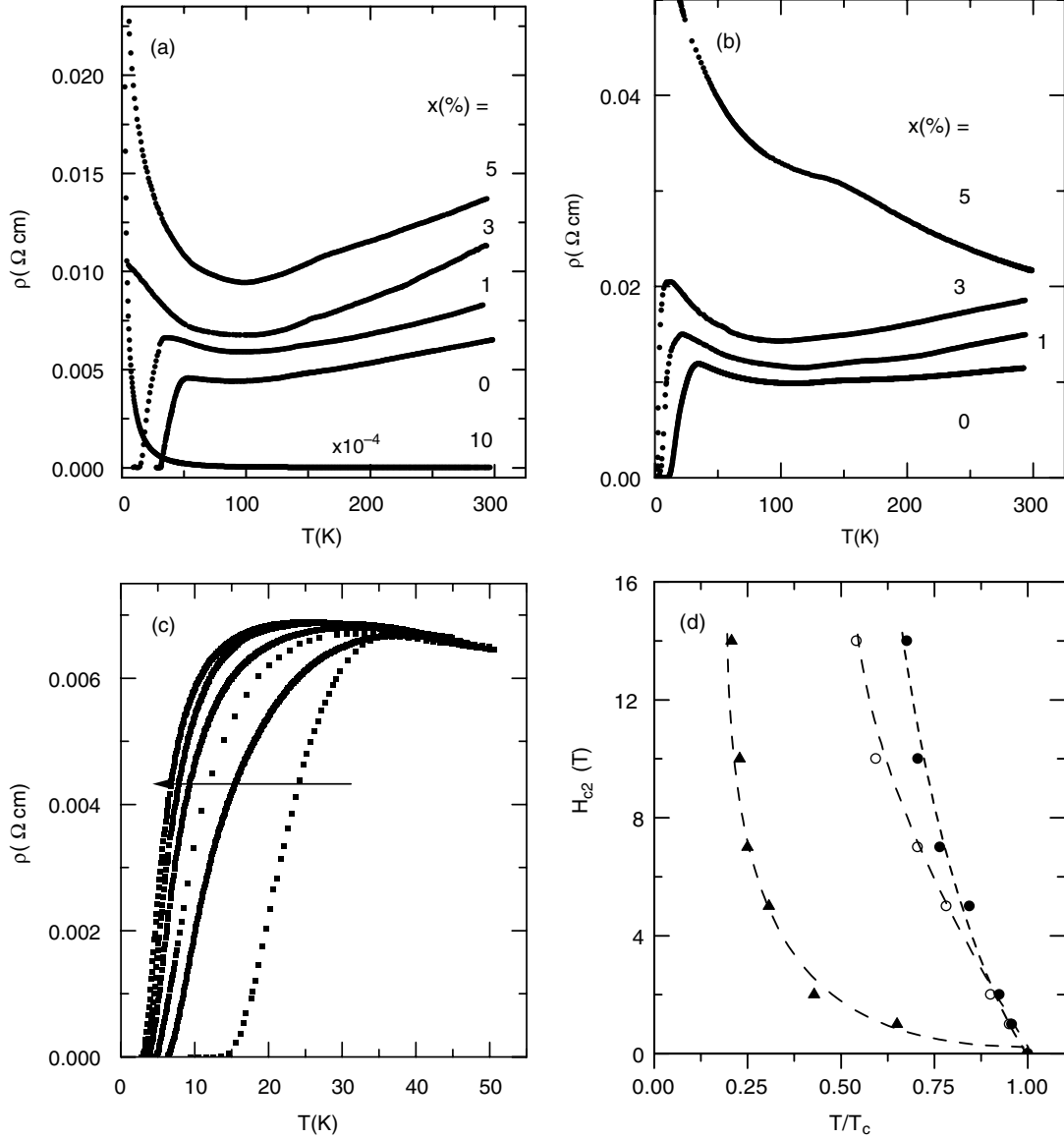


Fig. 1. (a) Temperature dependence of the resistivity for $\text{Ru}(\text{Sr}_{1-x}\text{La}_x)_2\text{GdCu}_2\text{O}_8$. (b) Temperature dependence of the resistivity for $\text{Ru}(\text{Sr}_{1-x}\text{La}_x)_2\text{EuCu}_2\text{O}_8$. (c) Temperature dependence of the resistivity for Gd-based sample with $x = 0.01$ at different magnetic fields (0, 2, 5, 7, 10 and 14 T). The arrow indicates the direction of increase of field. (d) The behavior of upper critical field $H_{c2}(T)$ determined from (c) using different criteria for T_c as described in the text: solid circles for T_c^{on} ; open circle for 90% of the normal-state resistivity and solid triangles for $T_c (R = 0)$. The dashed lines are guide to the eyes.

very different from that observed in liquid nitrogen quenched samples where T_c^{on} does not change but the transition width increases due to the enhancement of granularity [5]. The temperature dependence of ρ for $x = 0.03$ and 0.05 is similar to $x = 0$

sample but no superconductivity is observed down to 1.5 K. However, for $x = 0.03$ sample, $\rho(T)$ shows a change in slope at low temperatures and ρ decreases slightly below 1.5 K. This indicates that superconductivity appears for $x \leq 0.03$.

Normal-state resistivity is observed to increase monotonically with increasing x . For $x = 0.10$ sample, $\rho(T)$ shows semiconducting-like behavior over the whole range of temperature. The resistivity of this sample can be fitted with the standard expression for hopping conduction $\rho(T) = \rho_0 \exp(T_0/T)^n$, where ρ_0 , T_0 and n are constants. The conduction mechanism is dominated by nearest-neighbor-hopping (NNH) ($n \sim 1$) above 120 K and variable-range-hopping (VRH) ($n \sim 1/4$) below 65 K. Thus a crossover from VRH to NNH exists with increasing temperature as in the case of other HTSC.

It is clear from Fig. 1b that the evolution of transport properties and the suppression of superconductivity in $\text{Ru}(\text{Sr}_{1-x}\text{La}_x)_2\text{EuCu}_2\text{O}_8$ are qualitatively similar to that observed in La-doped RuGd-1212 . Though T_M for $\text{RuSr}_2\text{EuCu}_2\text{O}_8$ (RuEu-1212) sample is close to that for RuGd-1212 but T_c is much lower in the former system. For RuEu-1212 , ρ starts to decrease at around $T_c^{\text{on}} = 35$ K and becomes zero at $T_c^{R=0} = 12$ K. $x = 0.03$ sample shows superconductivity below 3 K. This may be due to the smaller value of La content in the sample than the nominal starting composition. In general Eu-based samples are more resistive than the Gd-based compounds with same x . The rapid suppression of superconductivity and the evolution of semiconducting-like state with small amount of La doping are typical of a strongly underdoped cuprate reflecting the depleted density of states near the Fermi level in ruthenate-cuprate.

The temperature dependence of resistivity at different magnetic fields is shown in Fig. 1c for $x = 0.01$ Gd-based sample. It is important to investigate the temperature dependence of upper critical field H_{c2} for this system because the superconducting state parameters, such as the upper critical field, flux pinning energy, etc., contain information about the superconducting condensation energy and probably is also related to the pairing mechanism of Cooper pairs. Mainly due to the effect of flux flow, a remarkable broadening of ρ as a function of T with increasing field is observed in high- T_c cuprates and hence a large uncertainty arises to define the T_c and to determine the H_{c2} . Normally, H_{c2} is determined from mag-

netization measurement. Due to the FM ordering of Ru moment it is difficult to determine H_{c2} from the magnetization measurements. In such cases, the determination of shift of the T_c from the temperature dependence of ρ in magnetic field is the principal method for determining H_{c2} . To avoid the effect of flux flow the temperature at which ρ starts to decrease from its normal value is defined as T_c^{on} for the estimation of H_{c2} . It is clear from Fig. 1c that the resistive broadening is not strong and no resistive tail appears at low temperatures. Also one can see that T_c ($R = 0$) at high fields shifts quite slowly towards lower temperatures. Qualitatively similar behavior of ρ has been observed for RuEu-1212 in applied magnetic field.

The variation of H_{c2} with temperature determined from different criteria is shown in Fig. 1d. H_{c2} determined from the shift of the transition temperature near the onset of superconductivity (as shown in Fig. 1d by solid and open circles) shows a steep slope with $dH_{c2}/dT \sim 1$ T/K. On the other hand, H_{c2} calculated from the field dependence of T_c ($R = 0$) shows a smaller slope near T_c , a positive curvature and a rapid increase as T approaches 0 K. Similar behavior has also been observed in some other overdoped HTSC [15,16]. The absence of resistive tail and the high value of H_{c2} suggest strong pinning force in this system. This indicates that the superconducting condensation energy due to pairing is large because the pinning energy is proportional to the square of condensation energy. The temperature dependence of H_{c2} for Ru-1212 is qualitatively similar to that observed in $\text{Bi}_2\text{Sr}_2\text{CuO}_6$ (Bi-2201) [17], $\text{La}_{2-x}\text{Sr}_x\text{CuO}_4$ (La-214) [17] and electron-doped systems [18]. In the Bi-2201 and La-214 systems, a second critical transition (T_{c2}) is observed well below T_c^{on} [17]. With increasing magnetic field, T_c^{on} decreases very slowly whereas T_{c2} decreases dramatically, showing a large positive curvature in the critical field.

Typical zero-field-cooled (zfc) susceptibility (χ) curves at $H = 0.5$ Oe for the Gd-based samples with $x = 0$, and 0.01 are shown in Fig. 2a. For $x = 0$ sample, a strong diamagnetic signal appears at around 28 K in the zfc cycle similar to that reported earlier [5]. The diamagnetic signal for $x = 0.01$ sample appears at much lower tempera-

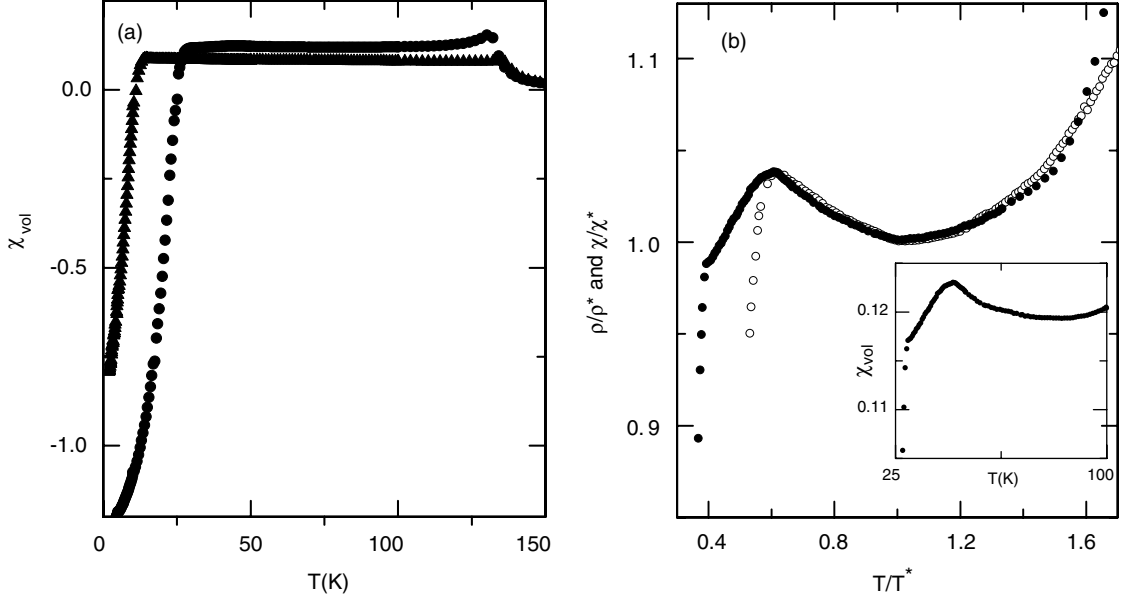


Fig. 2. (a) Temperature dependence of the zfc volume susceptibility at $H = 0.5$ Oe for RuGd-1212 for $x = 0$ (●) and 0.01 (▲). (b) The scaling behavior for the χ (zfc) and ρ for $x = 0$ sample as a function of reduced temperature T/T^* . Both χ and ρ were scaled to unity at their respective minimum. Inset shows the appearance of small diamagnetic signal in zfc cycle close to the resistive onset transition 46 K.

ture 12 K as compared to the pure sample. For both the samples diamagnetic shielding appears slightly below T_c ($R = 0$) and at low temperatures the volume fraction of the diamagnetic shielding without the demagnetization correction are $>100\%$ and 80% for $x = 0$ and 0.01, respectively. Such a large value of diamagnetic shielding suggests a bulk superconducting state for both the samples. However, the field-cooled susceptibility measurements show no sharp decrease of χ but a weak anomaly at the temperature where diamagnetic signal appears in the zfc cycle (not shown). A spontaneous vortex lattice (SVL) state or Fulde-Ferrel-Larkin-Ovchinnikov (FFLO) phase has been proposed [6,19] to form in a FM superconductor such that the internal magnetic field associated with the magnetic moment is greater than the lower critical field H_{c1} but smaller than the upper critical field H_{c2} . The formation of such SVL or FFLO-type phase can greatly reduce the size of the Meissner signal in the RuGd-1212 samples. For nonsuperconducting samples ($x \geq 0.03$), no diamagnetic signal has been observed down to 2

K. The T dependence of χ for these samples show an upturn at low temperatures similar to Zn-doped RuGd-1212 system. It is important to note that not only superconducting state properties but also the magnetic state of RuO_2 layers are strongly influenced by the La substitution. The magnetic transition is indicated by a cusp-like feature in the zfc cycles of χ .

Although the zfc susceptibility for $x = 0$ sample drops sharply at 28 K, closer inspection of the data on an expanded scale (inset to Fig. 2b) shows that a small amount of diamagnetic signal appears at around 46 K where resistivity drops sharply. This shows that the superconducting onset temperature is same for transport and magnetic measurements. Bernhard et al. [6] described the intermediate state between 28 and 46 K as a vortex phase. However, for $x = 0.01$ sample no diamagnetic signal has been detected close to the resistive onset temperature. Diamagnetic signal appears only below 12 K. We have already discussed that a two-step transition similar to RuGd-1212 has also been reported in Bi-2201 and La-214 systems [17]. In

these systems, χ decreases slowly from T_c^{on} down to the second critical transition and then decreases sharply below this temperature. Another interesting feature of $\chi(T)$ in RuGd-1212 is the occurrence of a shallow minimum at around T^* similar to that of $\rho(T)$. The T^* for $\chi(T)$ is about 10 K lower than that for $\rho(T)$. IR conductivity measurements [11] also revealed anomalies around T^* . Naturally, the question arises whether there is any common origin for the occurrence of this minimum. To address this question we have scaled both $\rho(T)$ and $\chi(T)$ to unity at their respective T^* and plotted as a function of reduced temperature T/T^* (Fig. 2b). Over a wide range of temperature both above and below T^* the data scale nicely indicating that T^* is a characteristic temperature of this system.

The temperature dependence of thermopower for La-doped RuGd-1212 and RuEu-1212 samples are shown in Fig. 3. A systematic evolution of S with temperature and La doping is clearly evident for both the systems. S increases with T , passes through a broad maximum (at T^S) and then decreases with further increase of temperature. At low temperatures below 160 K, S shows approxi-

mately linear T dependence, passes through the origin and the slope increases with the increase of x . With increasing x , the overall magnitude of S increases and T^S shifts towards higher temperature. The large value of S , the shape of $S(T)$ curve and the appearance of the broad maximum at high temperatures are the signatures of underdoped cuprates where normal-state transport properties including thermopower are strongly dominated by the presence of a pseudogap and the gap opening temperature increases with decreasing hole concentration [20]. The systematic increase of S and the shift of T^S towards higher temperatures with increasing x suggest that La is incorporated into the lattice and the system becomes more and more underdoped with increasing La concentration. The strong dependence of S on x also suggests that the suppression of superconductivity with La doping is not due to the effect of granularity as observed by Tallon et al. [5] for RuGd-1212 samples with different annealing conditions. We also compare the variation of S for the La-doped samples with that of the Zn-doped samples studied by Tallon et al. [5]. Superconductivity is strongly suppressed

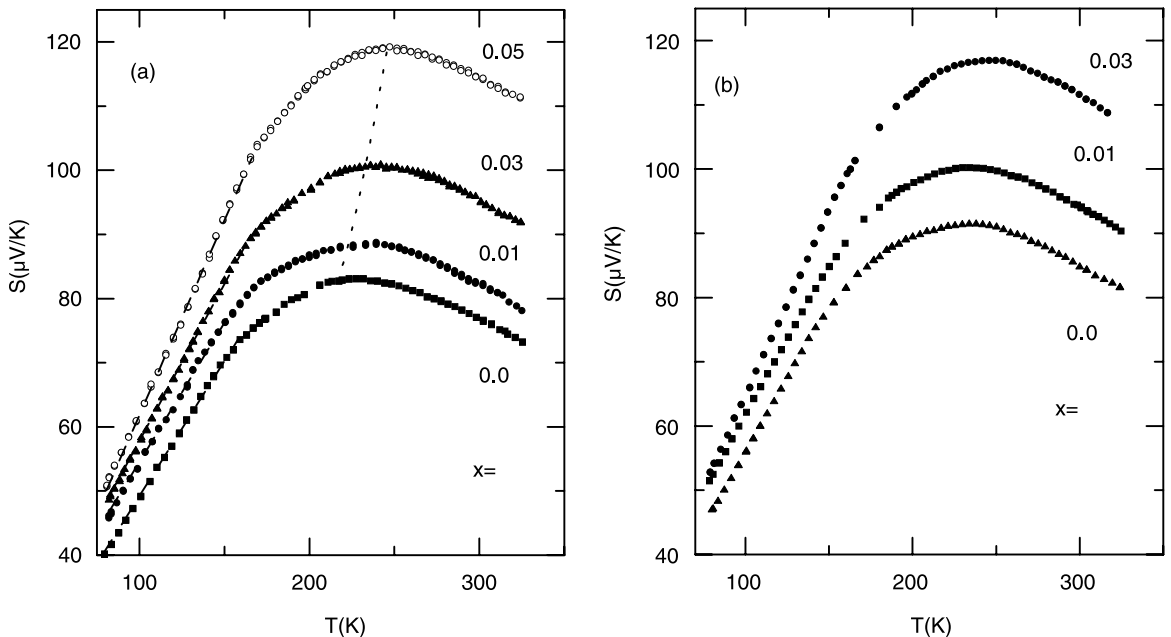


Fig. 3. Temperature dependence of the thermopower for different x . (a) Ru(Sr_{1-x}La_x)₂GdCu₂O₈ samples. The dashed lines indicate the linear behavior of S and the dotted curve shows the shift of the maximum with increasing x . (b) Ru(Sr_{1-x}La_x)₂EuCu₂O₈ samples.

with Zn doping similar to the present case while thermopower is almost unaffected by Zn substitution. Usually Zn suppresses superconductivity by introducing disorder in the CuO_2 planes maintaining the doping level almost same whereas La doping suppresses superconductivity by reducing carrier density in the system. It is worthwhile to compare RuGd-1212 with Y-123 because of their structural similarity. The CuO chain in Y-123, which is known as charge reservoir is replaced by RuO_2 plane in RuGd-1212. In Y-123 system, superconductivity disappears at around $\delta = 0.6$. Strikingly, both the magnitude and temperature dependence of S for RuGd-1212 are comparable to that of Y-123 system [20] close to $\delta = 0.6$. In HTSC a unique relation between p and room-temperature thermopower S (300 K) has been established [20]. If we assume that this relationship is also applicable for RuGd-1212 then $x = 0$ sample corresponds to $p \sim 0.07$ hole per Cu ion [5]. This indicates highly underdoped nature of RuGd-1212 which is consistent with the resistivity behavior. As substitution of one La ion reduces one hole per Cu ion, the complete suppression of superconductivity at around $x = 0.03$ corresponds to $p = 0.04/\text{Cu}$ ion. This value of p is close to the doping level for the occurrence of superconductivity in other cuprates and also close to that predicted by the well-known parabolic relation $T_c/T_c^{\text{max}} = 1 - 82.6 \times (p - 0.16)^2$ [12].

A general phase diagram, (T, x) , for RuGd-1212 is shown in Fig. 4. T_c is calculated at the mid-point of the superconducting transition of all doped samples. Superconductivity appears only in a narrow range of La^{3+} doping $x \leq 0.03$, while the magnetic ordering temperature was enhanced with increasing x up to 0.10. The dependence of T^* on x is also shown in this figure (thick solid line). In the temperature range between T^* and T_M the system exhibits weak FM metallic ($d\rho/dT > 0$) behavior and it is a paramagnetic metal above T_M . As T^* vs. x diverges above $x = 0.05$, both FM as well as paramagnetic state are insulating for these samples.

In conclusion, it has been possible to prepare ruthenate-cuprate samples with varying carrier concentration by successfully doping La in place of Sr in RuGd-1212 compound. Systematic variation of transport and magnetic properties in this

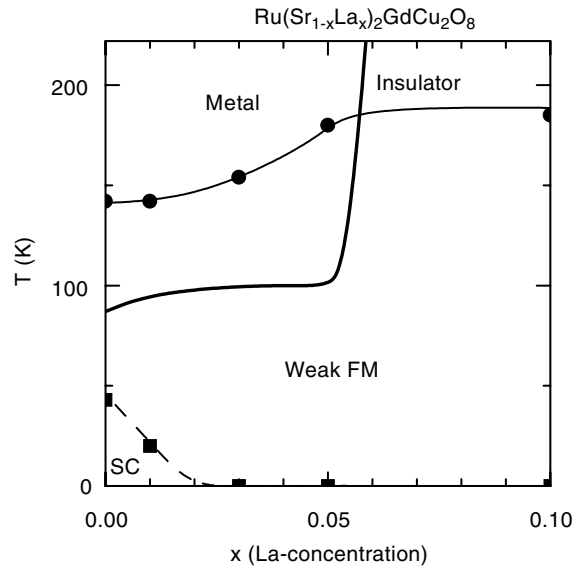


Fig. 4. Doping dependence of superconducting transition T_c (\blacksquare), FM transition T_M (\bullet) and T^* (—) for $\text{Ru}(\text{Sr}_{1-x}\text{La}_x)_2\text{GdCu}_2\text{O}_8$.

system has been studied as a function of La doping. With increasing x , T_c decreases considerably and the system becomes more and more underdoped. Superconductivity appears in the vicinity of insulator to metal transition point similar to other high- T_c materials.

Acknowledgements

We gratefully acknowledge the financial support from the Deutsche Forschungsgemeinschaft and Indian National Science Academy.

References

- [1] L. Bauernfeind, W. Widder, H.F. Braun, *Physica C* 254 (1995) 151.
- [2] I. Felner, U. Asaf, Y. Levi, O. Millo, *Phys. Rev. B* 55 (1997) R3374.
- [3] J.L. Tallon, C. Bernhard, M.E. Bowden, P.W. Gilberd, T.M. Stoto, D. Pringle, *IEEE Trans. Appl. Supercond.* 9 (1999) 1696.
- [4] C. Bernhard, J.L. Tallon, Ch. Niedermayer, Th. Blasius, A. Golnik, E. Brucher, R.K. Kremer, D.R. Noakes, C.E. Stronach, E.J. Ansaldo, *Phys. Rev. B* 59 (1999) 14099.

- [5] J.L. Tallon, J.W. Loram, G.V.M. Williams, C. Bernhard, *Phys. Rev. B* 61 (2000) R6471.
- [6] C. Bernhard, J.L. Tallon, E. Brücher, R.K. Kremer, *Phys. Rev. B* 61 (2000) R14960.
- [7] J.W. Lynn, B. Keimer, C. Ulrich, C. Bernhard, J.L. Tallon, *Phys. Rev. B* 61 (2000) R14964.
- [8] O. Chmaissem, J.D. Jorgensen, H. Shaked, P. Dollar, J.L. Tallon, *Phys. Rev. B* 61 (2000) 6401.
- [9] G.V.M. Williams, S. Krämer, *Phys. Rev. B* 62 (2000) 4132.
- [10] P. Mandal, A. Hassen, J. Hemberger, A. Krimmel, A. Loidl, *Phys. Rev. B* 65 (2002) 144506.
- [11] A.V. Boris, P. Mandal, C. Bernhard, N.N. Kovaleva, K. Pucher, J. Hemberger, A. Loidl, *Phys. Rev. B* 63 (2000) 184505.
- [12] M.R. Presland, J.L. Tallon, R.G. Buckley, R.S. Liu, N.E. Flower, *Physica C* 176 (1991) 95.
- [13] J.D. Jorgensen, O. Chmaissem, H. Shaked, S. Short, P.W. Klamut, B. Dabrowski, J.L. Tallon, *Phys. Rev. B* 63 (2001) 054440.
- [14] P. Mandal, A. Poddar, P. Choudhury, B. Ghosh, *Phys. Rev. B* 43 (1991) 13102.
- [15] A.P. Mackenzie, S.R. Julian, G.G. Lonzarich, A. Carrington, S.D. Hughes, R.S. Liu, D.S. Sinclair, *Phys. Rev. Lett.* 71 (1993) 1238.
- [16] M.S. Osofsky, R.J. Soulen Jr., S.A. Wolf, J.M. Broto, H. Rakoto, J.C. Ousset, G. Coffe, S. Askenazy, P. Pari, I. Bozovic, J.N. Eckstein, G.F. Virshup, *Phys. Rev. Lett.* 71 (1999) 2315.
- [17] H.H. Wen, X.H. Chen, W.L. Yang, Z.X. Zhao, *Phys. Rev. Lett.* 85 (2000) 2805;
H.H. Wen, W.L. Yang, Z.X. Zhao, Y.M. Ni, *Phys. Rev. Lett.* 82 (1999) 410.
- [18] Y. Dalichaouch, B.W. Lee, C.L. Seaman, J.T. Markert, M.B. Maple, *Phys. Rev. Lett.* 64 (1990) 599;
Y. Hidaka, M. Suzuki, *Nature (London)* 338 (1989) 635.
- [19] W.E. Pickett, R. Weht, A.B. Shick, *Phys. Rev. Lett.* 83 (1999) 3713.
- [20] D. Obertelli, J.R. Cooper, J.L. Tallon, *Phys. Rev. B* 46 (1992) 14928.